

Steven P. Oncley^{*1}, William J. Massman², Edward G. Patton¹

¹National Center for Atmospheric Research[†] Boulder, Colorado

²United States Forest Service, Rocky Mountain Research Station, Ft. Collins, Colorado

Abstract

Fast-response pressure fluctuations were included in the Canopy Horizontal Array of Turbulence Study (CHATS) at several heights within and just above the canopy in a walnut orchard. Two independent systems were intercompared and then separated. We present an evaluation of turbulence statistics – including the pressure transport term in the turbulence kinetic energy budget equation – within this canopy.

1 Introduction

Although pressure gradients in part drive atmospheric flows, relatively few observations of turbulent pressure fluctuations have been made. This is because it is difficult to design a pressure port that minimizes dynamic pressure effects and a high accuracy transducer is required. Wilczak and Bedard (2004) have a good discussion of many of the issues with pressure fluctuation measurements. Nevertheless, by now there are several port designs (Elliott, 1970 and Nishayama and Bedard, 1991) and transducers are commercially available that have enough resolution. Cuxart et al. deployed ports and transducers similar to those used here though with a different reference volume. They used a lower sampling rate (to obtain higher pressure resolution), but still attempted to obtain the TKE pressure transport term in the nocturnal boundary layer. A few studies have used these transducers to understand turbulent flow over relatively simple surfaces (short vegetation and water). Here we describe the first observations over a tall vegetation canopy.

Even without direct observations, several studies have described pressure fluctuations inside and just above a canopy. Fitzmaurice et al. (2004) used a large eddy simulation (LES) model of a forest canopy and showed that pressure fluctuations are largest in magnitude near the top of the canopy. Christen et al. (2008)

calculated the pressure transport term in the turbulence kinetic energy budget equation for a sparse coniferous canopy as a residual from measurements of all other TKE budget terms.

2 Instrumentation

Quad-disk probes (Nishiyama and Bedard, 1991) were used to avoid dynamic pressure errors. Ports made by NOAA/ETL were chosen based on wind tunnel testing of three versions of this design. Even these ports have errors that change from below 5% to above 50% as the attack angle changes from 20 to 30 degrees (see Fig 1). Therefore, use of the ports in the canopy (where turbulence intensity and thus instantaneous wind attack angles can be large) might require that much of the data be rejected. One port location was placed in the horizontal array and thus is expected to suffer from this problem, however the other was placed at approximately $1.1h$, where Li et al. (2004) found that turbulence intensity is less than inside the canopy.

Two types of sensors were connected to these ports, one now owned by the U.S. Forest Service (“USFS” below) similar to that described by Wilczak and Bedard (2004) that used an analog transducer and a reference volume with a calibrated leak, and another constructed by NCAR that used a digital transducer and a fixed reference volume with a thermal time constant of 45 minutes. Both sensors were deployed under a tarp to reduce radiative heating/cooling and the NCAR sensor was buried in the ground to reduce thermal forcing further. (A third, slower response, sensor also was deployed to verify the p' sensor operation at low frequencies.) Before being placed in their final locations, the systems were connected to the same pressure port and determined to be operating properly.

3 Deployment

The CHATS experiment has been described by Patton et al. (2008), so only a brief summary is given here. Two sets of towers were placed in a walnut orchard near Dixon, California with a canopy height of 10 m.

^{*}Corresponding author address: Steven P. Oncley, NCAR/ATD, P.O. Box 3000, Boulder, CO 80307-3000.

[†]The National Center for Atmospheric Research is supported by the National Science Foundation.

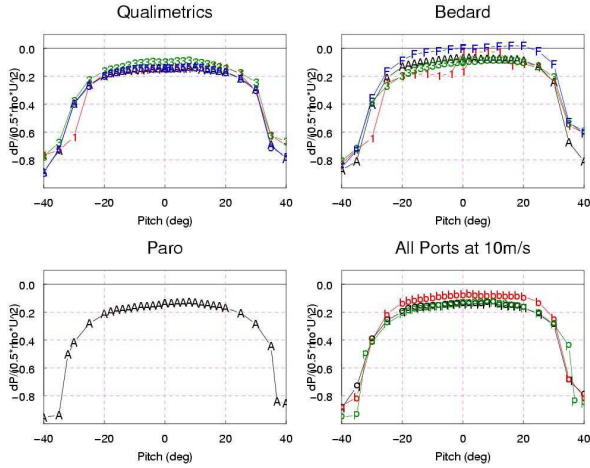


Figure 1: The dynamic error from three styles of quad-disk probes determined in a wind tunnel. The Qualimetrics and Bedard probes were tested at speeds of 1, 3, 10, and 15 m s⁻¹ (curves labeled “1”, “3”, “A”, and “F”, respectively) and the Paroscientific probe only at 10 m s⁻¹. Results from all three ports at 10 m s⁻¹ are shown in the lower right panel.

A tower structure supported a horizontal array of sonic anemometers that was moved between 3 sets of vertical levels within the canopy. A single 30 m tower was located 100 m to the north of the horizontal array. Both towers had a fetch of at least 1300 m over the orchard for the expected southerly winds.

Four locations for pressure inlets were used during this study. A port was placed just above the canopy at a height of 11 m on the 30 m tower, colocated with a three-component sonic anemometer. Both transducer systems were connected to this port by 16 April. On 12 May, another port was installed in the middle of the horizontal array and connected to the NCAR transducer. Throughout the rest of the CHATS program, this port was alternately placed at heights of 2.5, 5.4, and 10.1 m (along with the rest of the horizontal array), with sonic anemometers 0.5 m above and below the port.

4 Testing

4.1 NCAR/USFS Comparison

The NCAR and USFS sensors sampled the same port for almost a month, in order to check their performance. Figure 2 shows good agreement between the power spectra from these sensors from about 0.02 to 5 Hz. As expected, at lower frequencies, the USFS sensor loses energy due to high-pass filtering of the capil-

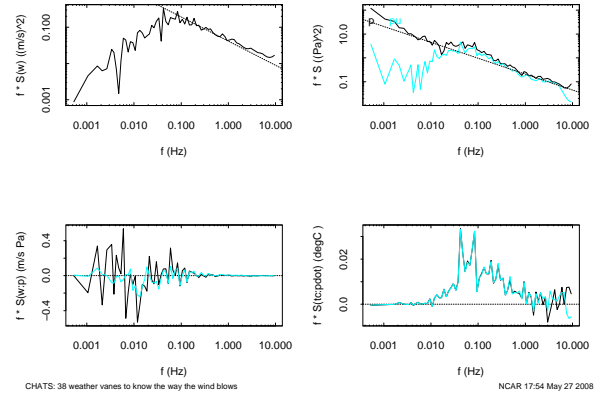


Figure 2: Power spectra of w (upper left) and p (upper right) and cospectra between w and p (lower left) and tc and dp/dt (lower right) for 30 minutes on the evening of 18 April. Data from the NCAR sensor are black lines and from the USFS sensor are blue.

lary leak on the transducer reference. Also, the NCAR sensor may have suffered from temperature changes at low frequencies. At high frequencies, the analog signal from USFS sensor was digitally low-pass filtered to reduce aliasing and the digital signal from the NCAR sensor suffered from discretization noise at low signal levels. Given this expected sensor behavior, the cospectra with w agree well, with more low-frequency energy seen in the NCAR sensor (but which appears to integrate to zero for both sensors). Since the time derivative of p is weighted towards high frequencies, the tc , dp/dt cospectra agree quite well, except at high frequencies. These results indicate that the p' sensors were responding appropriately.

4.2 Horizontal Heat Flux

Following Wilczak and Bedard (2004), we also checked the performance of these sensors using the horizontal heat flux budget. Clearly, Monin-Obukhov similarity relations are not applicable for these measurements close to and within a canopy, but the CHATS dataset contains enough information to compute each term of the budget (that is applicable for any flow) directly.

For horizontally-homogenous conditions, the normalized horizontal heat flux budget equation is:

$$0 = \phi_m + \phi_h + \phi_{hp} + \phi_{ht} \quad (1)$$

where

$$\phi_m = \frac{kz}{u_*} \frac{d\bar{U}}{dz}, \quad (2)$$

$$\phi_h = \frac{kz}{\theta_*} \frac{d\bar{\Theta}}{dz}, \quad (3)$$

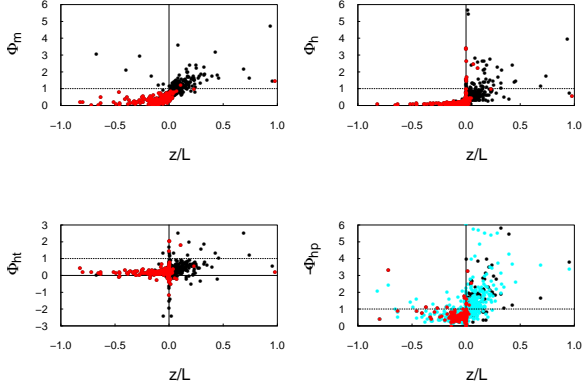


Figure 3: Terms of the horizontal heat flux budget shown as functions of z/L , where L is the Obukhov length. Black and red points are from the NCAR sensor and blue and magenta from the USFS sensor. Magenta and red values (almost all unstable data) are when the attack angles are large.

$$\phi_{ht} = \frac{kz}{u_*^2 \theta_*} \frac{d\overline{uw\theta}}{dz}, \quad (4)$$

and

$$\phi_{hp} = \frac{kz}{u_*^2 \theta_*} \frac{d\overline{\theta dp/dx}}{\rho}. \quad (5)$$

In these equations, p is the pressure, ρ is the density, ϵ is the dissipation of TKE, z is the measurement height, D is the displacement height, g is gravitational acceleration, k is the von Kármán constant, θ is the potential temperature, u_* is the friction velocity equal to $\sqrt{-\overline{uw}}$ and $\theta_* \equiv -\overline{w\theta}/u_*$. Note that ϕ_{hp} does not involve a derivative in z , so a separate determination may be made from only one measurement of θ and p .

Figure 3 shows that both ϕ_m and ϕ_h are smaller than values expected in the surface layer (as expected) and values for ϕ_{ht} are somewhat larger. However, Figure 4 shows that these terms are in a reasonable balance. The primary exception is for $\phi_m + \phi_h + \phi_{ht}$ less than 0.5, where ϕ_{hp} stays about constant at 0.5. These points, indicated in magenta and red, occur when a significant amount of the data have large attack angles and thus we expect erroneously large variance in p . Thus, we have some confidence that our measurements of p are reasonable for cases when the attack angle is not too large.

5 TKE budget

Under steady-state conditions, the normalized form of the TKE budget equation is

$$0 = \phi_m - \zeta - \phi_t - \phi_p - \phi_\epsilon \quad (6)$$

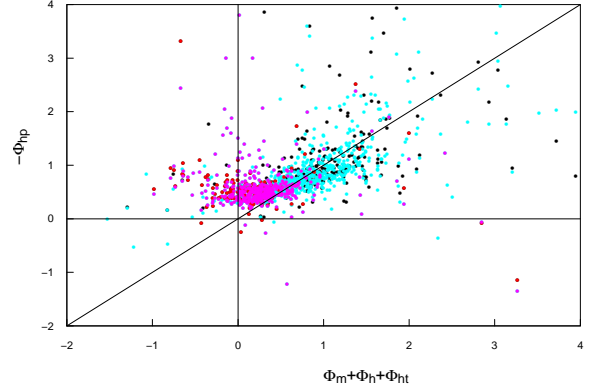


Figure 4: The horizontal heat flux balance. Colors are as for Fig. 3.

where

$$\zeta = \frac{-kzg\overline{w\theta_v}}{u_*^3 \Theta_v} \equiv \frac{z}{L}; \quad L \equiv \frac{-u_*^3 \Theta_v}{kgw\theta_v} \quad (7)$$

$$\phi_t = \frac{kz}{u_*^3} \frac{d}{dz} \frac{\overline{wq}}{2} \quad (8)$$

$$\phi_p = \frac{kz}{u_*^3} \frac{d}{dz} \frac{\overline{wp}}{\rho_o} \quad (9)$$

and

$$\phi_\epsilon = \frac{kz}{u_*^3} \epsilon \quad (10)$$

where ϵ is the dissipation rate of TKE. We would like to obtain an estimate of ϕ_p from these data, however only two pressure sensors were used and they were deployed on different towers. Nevertheless, we can present values of $\overline{w'p'}$ as a function of height (Fig. 5). In this figure, we normalize values of $\overline{w'p'}$ at the various heights in the horizontal array by the measurement at 11 m. The result is in general agreement with Fig. 7 of Dwyer et al. (1997). The vertical gradients in $\overline{w'p'}$ are small (and thus ϕ_p is small) in the bottom of the subcanopy space. From the mid canopy to near the canopy top, $\overline{w'p'}$ (and ϕ_p) increases. Near the canopy top, $\overline{w'p'}$ is nearly constant with height, so ϕ_p would drop to close to zero.

6 Summary

The pressure fluctuations measured during CHATS appear to be of reasonable quality. However, in and near the canopy, the flow had instantaneous attack angles occurred that were outside the (reasonably large) acceptable range of the pressure ports that were used. Nevertheless, over 150 hours of data have been found

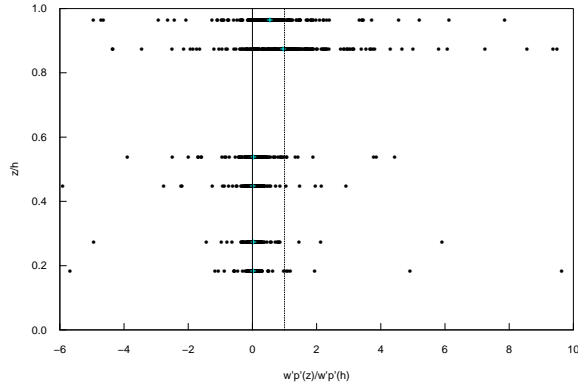


Figure 5: Values of $\overline{w'p'}$ within the horizontal array normalized by the values measured at 11 m shown as a function of z normalized by the canopy height h . Values are shown calculated using both the w above and below the p measurement. Blue crosses show the median of all the values at each level.

that satisfy the criterion of a balanced horizontal heat flux. Using these data, we have started to estimate the pressure transport term in the TKE budget and find that it qualitatively agrees with previous LES results. However, more data analysis is needed to determine if quantitative agreement is obtained.

Acknowledgements

We are grateful to the owners and staff of Cilker Orchards for allowing CHATS to occur and for providing logistical support. Primary funding for CHATS was provided by the National Science Foundation. Support for the pressure measurements was provided by The Institute for Integrative and Multidisciplinary Earth Studies (TIIMES) at NCAR. The National Center for Atmospheric Research is sponsored by the National Science Foundation. Any opinions, findings and conclusions or recommendations expressed in this publication are those of the authors and do not necessarily reflect the views of the National Science Foundation.

References

Christen, A., M. Novak, T.A. Black, and M. Brown, 2008, "The budgets of turbulent kinetic energy and sensible heat flux within and above a sparse lodgepole pine stand", 28th Conference on Agricultural and Forest Meteorology, American Meteorological Society, Orlando, Florida, 28 April – 2 May, **J2.7**.

- Cuxart, J., G. Morales, E. Terradellas, and C. Yagüe, 2002, "Study of coherent structures and estimation of the pressure transport terms for the nocturnal stable boundary layer", *Bound.-Layer Meteor.*, **105**, 305–328.
- Dwyer, M.J., E.G. Patton, R.H. Shaw, 1997, "Turbulent kinetic energy budgets from a large-eddy simulation of flow above and within a forest canopy", *Bound.-Layer Meteor.*, **84**, 23–43.
- Elliott, J.A., 1970, "Microscale pressure fluctuations measured within the lower atmospheric boundary layer", Ph.D. dissertation, University of British Columbia, 195 pp.
- Fitzmaurice, L., R.H. Shaw, K.T. Paw U, E.G. Patton, 2004, "Three-dimensional scalar microfront systems in a large-eddy simulation of vegetation canopy flow", *Bound.-Layer Meteor.*, **112**, 107–127.
- Nishiyama, R.T. and A.J. Bedard, Jr., 1991, "A quad-disk static pressure probe for measurement in adverse atmospheres - With a comparative review of static pressure probe designs", *Rev. Sci. Instrum.*, **62**, 2193–2204.
- Patton, E.G., T.W. Horst, D.H. Lenschow, P.P. Sullivan, S.P. Oncley, S.P. Burns, A. Guenther, A. Held, T. Karl, S. Mayor, L. Rizzo, S. Spuler, J. Sun, A. Turnipseed, E. Allwine, S. Edburg, B. Lamb, R. Avissar, H.E. Holder, R. Calhoun, 2008, "The Canopy Horizontal Array Turbulence Study (CHATS)", *Bull. Amer. Meteorol. Soc.*, **in prep**.
- Wilczak, J.M. and A.J. Bedard, Jr., 2004, "A new turbulence microbarometer and its evaluation using the budget of horizontal heat flux", *J. Atmos. Ocean. Tech.*, **21**, 1170–1181.